Automatic generation of semantically rich as-built building information models using 2D images: A derivative-free optimization approach

Fan Xue, Weisheng Lu* & Ke Chen

Department of Real Estate and Construction, The University of Hong Kong, Pokfulam, Hong Kong SAR

Abstract: *Over the past decade a considerable number of studies have focused on generating semantically rich as-built building information models (BIMs). However, the prevailing methods rely on laborious manual segmentation or automatic but error-prone segmentation. In addition, the methods failed to make good use of existing semantics sources. This paper presents a novel segmentation-free derivative-free optimization (DFO) approach that translates the generation of as-built BIMs from 2D images into an optimization problem of fitting BIM components regarding architectural and topological constraints. The semantics of the BIMs are subsequently enriched by linking the fitted components with existing semantics sources. The approach was prototyped in two experiments using an outdoor and an indoor case, respectively. The results showed that in the outdoor case 12 out of 13 BIM components were correctly generated within 1.5 hours, and in the indoor case all target BIM components were correctly generated with a root-mean-square deviation (RMSD) of 3.9 cm in about 2.5 hours. The main computational novelties of this study are: (a) to translate the automatic as-built BIM generation from 2D images as an optimization problem; (b) to develop an effective and segmentation-free approach that is fundamentally different from prevailing methods; and (c) to exploit online open BIM component information for semantic enrichment, which, to a certain extent, alleviates the dilemma between information inadequacy and information overload in BIM development.*

1 INTRODUCTION

This paper presents an effective approach for automatic generation of semantically rich as-built building information models (BIMs). According to the National BIM Standard of United States (NIBS, 2015), a BIM is the digital representation of physical and functional characteristics of a facility. BIM forms a shared knowledge resource for information about a facility, serving as a reliable basis for decisions making (NIBS, 2015). An as-built BIM refers to a digital representation of the facility as it was actually built or as it currently exists. Generally, there are two types of semantic information contained in a BIM (e.g., Eastman et al., 2011; NIBS, 2015; Belsky et al., 2016).

1. Semantic information of individual construction components, including:
   a. Geometric information, such as size, position, shape and textures; and
   b. Non-geometric information, such as type, specifications of material, and meanings of functions.
2. Semantic information of relationships between components, such as dependency, topology, and joint information.

Some critical semantic information, such as *actual* building geometries, *current* functions, and *real* topology of facilities, are only embodied in as-built BIMs (Tang et al., 2010; Pătrăucean et al., 2015). Semantically rich as-built BIMs can enable many value-added applications, including facility management (Becerik-Gerber et al., 2011), building

*To whom correspondence should be addressed. E-mail: wilsonlu@hku.hk.

retrofitting and renovation (Ilter and Ergen, 2015), and energy consumption simulation (Cho et al., 2015). Generation of such BIMs has therefore attracted the interest of practitioners and academics in the architecture, engineering, construction, and operations industry.

Only a few buildings currently have a digital representation of their as-built condition in the form of BIM. For a constructed facility, the BIM created at the design stage does not adequately represent the most updated condition of a building due to design changes, inadvertent deviations or errors, and renovation work; to do so, the as-designed BIM needs to be updated into an as-built BIM (Chen et al., 2015; Hamledari et al., 2017). To manually label the semantic information onto a BIM is possible but extremely tedious and time-consuming. Researchers have thus endeavored to achieve such semantically rich as-built BIMs by developing various automatic modeling approaches over the past decade. Laser scanning and photogrammetry were adopted with a view to rapidly surveying digital measurements (e.g., point clouds or imagery) as the raw data that can be preprocessed for subsequent modeling. Considerable progress has also been made in enhancing data preparations (e.g., Song et al., 2014; Zhang et al., 2016), developing data preprocessing algorithms, exploring model generation methods (e.g., Bosché et al., 2015; Díaz-Vilariño et al., 2015), and data transfer plan and rule-based inference for topological semantic enrichment (Hamledari et al., 2017; Sacks et al., 2017).

However, significant difficulties remain in the field of as-built BIM generation. For example, apart from their relatively high cost, point clouds and imagery primarily represent the geometric data of surfaces, which makes it extremely difficult to reveal the volumetric components and discover non-geometric semantics from the surfaces. Although segmentation methods based on *a priori* heuristic rules and up-to-date object recognition methods, such as *support vector machine* (SVM) (Adan and Huber, 2011; Perez-Perez et al., 2016), are developed for semantic enrichment, the overall results are generally unsatisfactory. Much manual work is still required to model the measurement into components, and in turn, to fit into an as-built BIM (Jung et al., 2014). On the other hand, many commercial or non-commercial organizations have started to publish semantic BIM components online for users to retrieve. For instance, more than 200,000 parametric BIM components are freely available on BIMobjects.com. Some researchers also started to develop specific sets such as the historical architectural BIM components by Santagati and Turco (2017). Such BIM components are well designed, rich in semantic information, and maintained by their industrial manufacturers. Clearly, there is a dilemma between information inadequacy and information overload in generating as-built BIMs.

It would constitute a novel proposition to recognize BIM components from the measured as-built conditions, and enrich their semantics by exploiting the information available in BIM components openly accessible online or elsewhere. Through this, it can also deal with the aforementioned information dilemma to a certain extent. The major difficulty is the BIM component recognition process, which involves burdensome manual segmentation, and huge amounts of computation, e.g., every component may have up to nine parameters of geometric degrees of freedom (position, scaling, and rotation in 3D) to determine regardless of topological and architectural requirements. The difficulty, nevertheless, can be controlled by harnessing powerful computational devices and advanced algorithms that have been successfully implemented to solve some extremely challenging scientific and engineering problems. Examples of such problems include the protein structure prediction (Nicosia and Stracquadanio, 2008), aircraft wings design (Lee et al., 2008), and surgical planning and treatment design (Clancey and Witten, 2011). All these challenging problems can be modeled and solved as optimization problems, for which many off-the-peg evolutionary computations and *derivative-free optimization* (DFO) methods have been developed in applied mathematics and computer science and applied to solve many engineering problems (Eiben and Smith, 2003; Conn et al., 2009). Regarding as-built BIM generation, architectural knowledge such as building styles (e.g., Baroque architecture) and structural regularity (e.g., flatness, parallels, and symmetries) can also be applied as constraints to effectively reduce the search space of the formulated problem (Chen et al., 2017).

This paper develops a DFO approach for the automated generation of semantically rich as-built BIMs using 2D images. The approach introduces three novelties that can significantly improve the field. Firstly, it formulates the as-built BIM generation as a constrained optimization problem, so that many established DFO algorithms can be applied to solve the problem. Secondly, the approach integrates the cutting-edge multidisciplinary instruments such as computer vision metrics and DFO algorithms to realize an effective and segmentation-free BIM generation approach. Thirdly, the approach makes good use of the architecture domain knowledge and rich semantics in BIM component libraries that are available on the Internet or elsewhere.

The remainder of the paper is structured into five sections. Section 2 reviews the literature on as-built BIM generation and DFO applications in related problems. Section 3 presents the proposed methodology. Section 4 describes the experimental tests of the proposed methodology wherein a BIM is rebuilt from a single picture of the building shot a considerable time ago and another one from two photos of a furniture store. Section 5 comprehensively discusses the advantages, shortcomings,

and future developments of the proposed method. Section 6 concludes the study and provides recommendations for future research.

2 LITERATURE REVIEW

2.1 Generation of as-built BIMs

Capturing the as-built conditions of a building is the foremost step for as-built BIM generation. This is traditionally conducted using conventional tape measurements by skilled persons. This manual process is extremely tedious, intensive, time-consuming, and at times, inaccurate. Nowadays, non-contact devices including ground-level *simultaneous localization and mapping* (SLAM) sensors (Nüchter, 2008), cameras on unmanned aerial vehicles (a.k.a. drones) (Dai and Lu, 2010; Nex and Remondino, 2014), ground and airborne laser scanners (Tang et al., 2010; Holgado-Barco et al., 2017), and satellite orbit-level synthetic aperture radars (Zhu and Shahzad, 2014) have been adopted for rapid as-built geometry measurements. Data captured by such measurement technologies is usually in the form of point cloud or a set of images. Furthermore, imagery can be processed into 3D point clouds using *Structure from Motion* (SfM) by estimating camera parameters and 3D structural information of scenes (Snavely et al., 2008). Vice versa, 3D point clouds can also be converted to 2D images, e.g., for lossless data compression (Houshiar and Nüchter, 2015) and as-built surface patches (Henry et al., 2012).

Methods for generating as-built BIMs from the measurement data can be categorized as either data-driven or model-driven. A data-driven method is to perform modeling based on the preprocessed measurement data. Valero et al. (2012) presented an automatic method that yields boundary representation models of indoor environments containing a variety of clutter; however, they estimate structural lines of indoor environments by the intersection of two adjacent planes, which is not a mathematically rigorous approach. *Ad-hoc* surface fitting heuristics such as improved *random sample consensus* (RANSAC) (Schnabel et al., 2007; Lagüela et al., 2013) and parametric curved surfaces (Zhang et al., 2015; Dimitrov et al., 2016) are employed to segment expected surfaces from real world noisy data. Object recognition and machine learning techniques such as SVM (Adan and Huber, 2011; Koppula et al., 2011; Perez-Perez et al., 2016; Wang et al., 2017) and convolutional neural networks (Babacan et al., 2017) are also adapted to identify semantic labels. Regarding directly generating BIM from images by using data-driven methods, Criminisi et al. (2000) applied projective geometrical techniques to create a 3D surface of the building shown in a single image. Wang et al. (2011) used hue, saturation, and value color space and red, green, and blue color segmentation to recognize and extract basic geometric information of house envelopes from the images

of the house. Quintana et al. (2018) combined color (RGB) from images and geometry (*xyz*) from point clouds to detect open, semi-open and closed doors.

Model-driven methods have also been explored. They generally refer to comparing the known components against the datasets (e.g., point clouds or imagery), recognizing components, and fitting them in a BIM based on pre-defined rules. The pre-defined rules could be known knowledge of digital building models/components (e.g., windows, doors, and beams) and their topographic constraints (e.g., a window should be embedded in the wall). Faber and Fisher (2002) considered the constrained surface optimization based on the *mean square error* (MSE) and employed a *genetic algorithm* (GA) to recognize parametric models from a doorway point cloud. Xiong and Huber (2010) encoded the point clouds into a voxel structure and detected planar patches by grouping neighboring points together using a region-growing method. This approach is further improved in Xiong et al. (2013), who introduced a context-based method to identify and model the structural components without projection of point clouds. Dore and Murphy (2014) presented a semi-automatic method for as-built BIM facade reconstruction. Their method first developed parametric facade template and estimated the position and size of the facade structure by classical architectural proportions. Then, users could manually edit the position, size, and other parameters of the generated facade.

Acknowledging previous efforts on as-built BIM generation, both data-driven and model-driven methods rely heavily on segmentation of measurement data, which is extremely error-prone (Tang et al., 2010; Pătrăucean et al., 2015; Perez-Perez et al., 2016). For instance, Koppula et al. (2011) achieved an about 80% precision and 70% recall with SVM in segmenting office scenes and an about 50% precision and 50% recall for home scenes. Babacan et al. (2017) found the precision of segmentation by deep learning varied from about 40% for beams to over 90% for walls and floors, recall varied from about 55% for doors to 99% for floors. In general, the generalization of computerized object recognition methods in the uncontrolled environments of real-life scenarios can often be unsatisfactory (Andreopoulos and Tsotsos, 2013). As a result, the reliance on segmentation often undermines the semantic enrichment level of prevailing as-built BIM development methods (Pătrăucean et al., 2015) and could indirectly raise the requirements (e.g., sufficient coverage, accuracy, and details) on the measurement data (Anil et al., 2013; Zhang et al., 2016).

In addition, a dilemma with as-built BIM generation is that on one hand there is a lack of semantic information in as-built BIMs, while on the other hand there is a plethora of semantic information on various BIM components that are available on the Internet or from other sources. This dilemma could be addressed by stitching the semantics in

various BIM components onto the as-built BIMs for semantic enrichment.

2.2 Derivative-free optimization applications in related problems

Many problems in civil and infrastructural engineering, such as optimal design of a structure (Adeli and Kamal, 1986) and fitting a parametric model to a point cloud (Fisher, 2004), can be modeled and solved as constrained optimization problems, in which there are constraints on the variables (Gill et al., 1981). Such a constrained optimization is a typical *NP*-hard (non-deterministic polynomial time hard) problem, which refers to a set of challenges whose solutions can be verified in polynomial time. Furthermore, fitting a single component (i.e., its multiple real parameters) with the measurement can be rather expensive in terms of the computational cost (see Aster et al., 2013); normally one will engage a third-party BIM platform to project a 3D BIM into 2D images, and mobilize the platform to perform the operations such as appending, relocating, scaling, and connecting until the best (or satisfactory) settlement of the BIM component is found. As these problems imply that traditional mathematical programs, such as IBM CPLEX and Gurobi Optimization, cannot be applied, a DFO solution is therefore demanded.

Examples of DFO algorithms for the constrained optimization problem include GA and *covariance matrix adaptation with evolution strategy* (CMA-ES). GA is a well-known algorithm for solving both constrained and unconstrained optimization problems. GA relies on operators of selection, mutation, and crossover on 'chromosomes' of independent variables, and mimics a natural selection process that drives biological evolution. Due to the complexity of real problems in civil engineering, parallel GAs were often employed, e.g., Adeli and Cheng (1994) demonstrated a parallel GA for 7.7 times of speed and Adeli and Kumar (1995) later used 512 CPUs for optimizing a structure consisting of 4,016 structural elements in parallel GAs. Some recent GA applications can be found as Li et al. (2017)'s optimal mountain railway alignment and Koo et al. (2016)'s optimal balances between time–cost–environment in vertical transportation for workers. CMA-ES (Hansen and Ostermeier, 2001; Hansen, 2016) incorporates evolution processes like GA. The difference is that CMA-ES also concerns pairwise dependencies between variables, i.e., the covariance matrix. Adaptation of the covariance matrix generally leads to optimizing a meta-model of the objective function. Therefore, although both are established algorithms, CMA-ES usually finds better solutions than GA for expensive objective functions (Hansen et al., 2010). For instance, Kaveh et al. (2011) applied CMA-ES on the optimal truss structure design problem and reported considerable improvements than the results from GA, e.g., a 31% improvement on the optimal design of weight for a 26-

story-tower space truss in less than one hour. Athanasiou et al. (2011) also applied CMA-ES in earthquake engineering, and obtained an improvement up to 53% compared to the previous solutions in the literature. In summary, the DFO methods have proven a strong capability in solving the challenging civil engineering problems.

Nevertheless, only a few references have been applied DFO methods to the generation of as-built BIMs. Faber and Fisher (2002) and Fisher (2004) set up an MSE-based objective function on point clouds and adapted GA in solving the formulated problem. As far as is concerned, the formulation of image-based generation of as-built BIM and the application of modern DFO methods such as CMA-ES have not been reported in the literature.

All these opportunities and challenges have engendered this study, which has developed an as-built BIM generation method that is segmentation-free, and can make use of existing information resources to generate a semantically rich BIM.

3 METHODOLOGY

3.1 Theoretical stance

The theoretical foundation of this study is to perceive the as-built BIM generation as a process of fitting the BIM components (e.g., facades, doors, windows), whereby the fitting task of each component is equivalent to solving a small-scale constrained optimization problem. In this study, the variables of the constrained optimization problem are the parameters of location, scaling, rotation, and topology of the BIM components. The objective function is to maximize the similarity between the measurement of as-built conditions and the target BIM model (a combination of the fitted components *per se*). The constraints over the variables are derived from the topological requirements between the components and the reasonable ranges of the component's parameters.

3.2 Problem formulation

Figure 1 illustrates how as-built BIM generation is translated in this research. There are two inputs of the constrained optimization problem: the measurement data of as-built conditions and the BIM components contained in libraries. The measurement data, in this paper, are 2D images that can be taken at a relatively low cost. These images should be meaningful, i.e., bird-view images are preferred for as-built rooftop modeling and front-view images for as-built facade modeling. Another input is the BIM components (e.g., facade, wall, windows, and doors) organized in one or multiple libraries. The semantics involved in this study come from two sources. One source is the optimized parameters of the digital BIM component, including the location, scaling, rotation, and topology, which are gradually obtained during the problem solving.
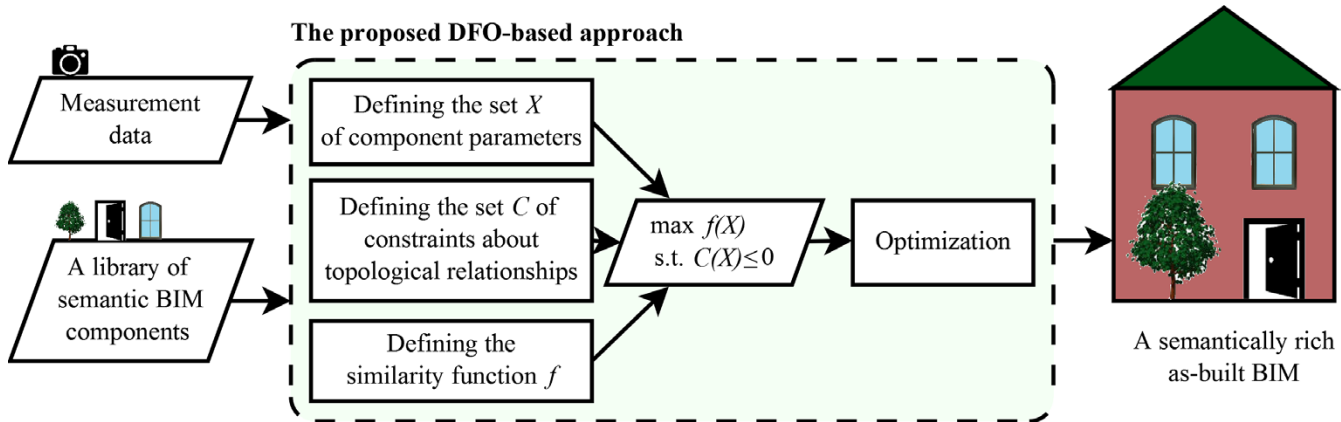
Figure 1 General framework of the DFO approach for as-built BIM generation

We define them in a tuple X_i for the i-th component instance:

$$X_i = (cl, l, s, r_z), \tag{1}$$

where cl is the class of the component (e.g., a three-section window), l is the 3D location, s is the 3D scaling, and r_z is the rotation around z-axis. Using mathematical language above, they are the *variables* of the constrained optimization problem. In view of the fact that not all components are relevant to a certain measurement, some rules based on architectural style and date of construction (e.g., Baroque architecture in 1910s) can be defined to filter irrelevant components. This filtering can significantly reduce the computational load. Another source of semantic information is the adoption of semantics from BIM component libraries. The categories of adopted semantics include surface pattern, architecture style, typical functions, materials, and mechanical properties.

The similarity function is the *objective function* of the constrained optimization problem. A similarity function measures the level of resemblance between the measurements as the input and the generated BIM. The importance of the similarity function is easy to understand, as the rationale of the methodology is to fit existing BIM components (by optimizing X_i) to the input measurement until a maximum/satisfactory similarity is achieved. Thanks to previous research in computer vision and pattern recognition, many such functions have been developed. For example, given an input imagery measurement and a BIM, a well-known similarity function is Wang et al. (2004)'s *structural similarity* (SSIM) index, which integrates structure, luminance, and contrast to compare two 2D images:

$$SSIM = structure \cdot luminance \cdot contrast$$

$$= \frac{(2\mu_{\hat{A}}\mu_A + c_1)(2\sigma_{\hat{A}A} + c_1)}{(\mu_{\hat{A}}^2 + \mu_A^2 + c_1)(\sigma_{\hat{A}}^2 + \sigma_A^2 + c_2)}, \tag{2}$$
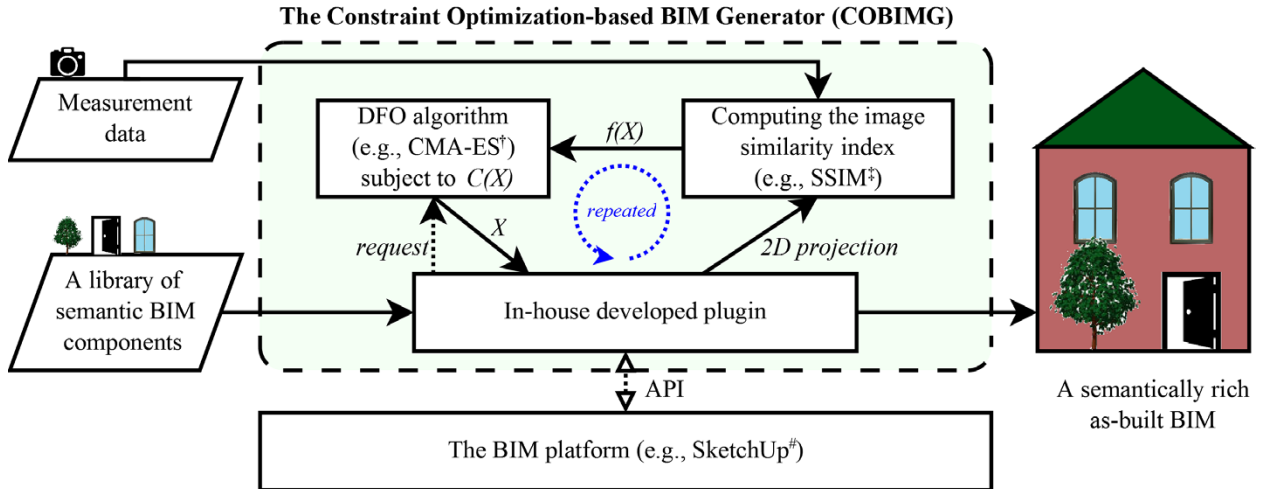
where A is the matrix of pixels in the input image, $\hat{A}$ is the matrix of pixels in 2D projection of the BIM to be

generated, μ_A and $\mu_{\hat{A}}$ are the means of A and $\hat{A}$, σ_A and $\sigma_{\hat{A}}$ are the standard deviations, $\sigma_{\hat{A}A}$ is the covariance, and c_1 and c_2 are two constants. It should be noted that BIM components are in 3D format and need to be projected into 2D images before the similarity test. SSIM was proven more accurate than conventional metrics such as MSE in measuring similarity of images (Wang and Simoncelli, 2008), since it considers not only the value of individual pixels, but also the structural arrangement of these pixels.

The optimization process to generate the semantically rich as-built BIM would be ineffective if the computations are not constrained. The constraints are derived from the topological requirements between components (e.g., a window must reside on a wall), the scale ranges of the components (e.g., the window should not be larger than the wall), as well as architecture conventions. Here, architectural conventions refer to the domain knowledge applied in the architectural design, such as building styles (e.g., Baroque architecture), geometrical or physical features (e.g., flatness, parallels, and symmetries) of building objects and their spatial relationships (Cantzler, 2003). Regardless of multiple appearances of architecture designs, there are only a limited types of topological relationships between building components in real life, including adjacency (e.g., *above*, *below*, and *next-to*), separation, containment, intersection, and connectivity (Nguyen et al., 2005). In this study, these types of topological relationships are employed to organize the constraints between components. The constraints C can be defined as a set of functions:

$$C(X) = \{C_I(X_i)\} \cup \{C_R(X_i, X_j), i \neq j\}, \tag{3}$$

where C_I indicates the constraints on the parameters X_i of any individual component, and C_R is the constraints on the topological relationships between any pair of (i-th, j-th) components. Examples of the two groups of constraints can be found in Table 1.

The Constraint Optimization-based BIM Generator (COBIMG)

†: In C++, supported by libcmaes (version 0.9.5, available at: https://github.com/beniz/libcmaes)
‡: In C++, supported by OpenCV (version 2.4.13, available at: http://www.opencv.org/)
#: Ruby API (version 2016 PRO, documentations available at: http://ruby.sketchup.com/)

Figure 2 Modules, supporting software libraries, and the DFO-based problem-solving process of COBIMG

Table 1
Example of constraints on individual component and topological relationships

C	Example	Example value	Notes
C_I	scaling_max	[1.5, 1.5, 1.5]	xyz coordinates
	scaling_min	[0.8, 0.8, 0.8]	Ibid.
	z_rotation_max	$\pi/2$	
	z_rotation_min	0	
C_R	on_top_of	'Ground'	Adjacency, connectivity
	contains_on	'Wall'	Containment or intersection
	min_separation	'0.5 m'	Separation

When all the *variables*, *objective functions*, and *constraints* are defined, the constrained optimization problem of as-built BIM generation can be expressed in the general form as:

$$\text{maximize} \quad f(X) = SSIM$$
$$\text{subject to} \quad C(X) \leq 0. \tag{4}$$

For researchers who tend to treat a minimization problem as the standard form, the objective function can be derived by negating the SSIM in Eq. (4).

3.3 Problem solving with software implementation

In order to implement the proposed method and solve the formulated problem in Sections 3.1 and 3.2, the authors developed an open-source software library *constrained optimization-based BIM generator* (COBIMG, source code and tutorials available at: https://github.com/ffxue/cobimg). As shown in Figure 2, COBIMG has three major modules. The first module is the DFO algorithm (e.g., CMA-ES) at the core. The second module is the similarity indexes (e.g., SSIM) to compare the projected image with the input

measurement. The third module is a set of plugins for manipulating components in different BIM platforms, including plugins for positioning, scaling, and projecting.

The problem-solving of COBIMG is a fully automatic, repetitive trial-and-error procedure as illustrated in Figure 2. The input BIM components could be Autodesk Revit's (.rfa format) or Trimble SketchUp's (.skp format), which provides the parameters and semantics, such as those listed in Table 1, of the components. Figure 3 shows the detailed operations and interactions between the modules of COBIMG in an individual trial for the i-th BIM component, using CMA-ES and SSIM as an example. At the start of the trial, the CMA-ES populates a feasible X_i that does not violate the constraints, e.g., the rotation r_z may not exceed the preset range. The plugin decodes from X_i to the parameters (e.g., location, scaling, rotation, and topology) of the i-th BIM component. Then, the BIM platform is instructed to manipulate the component as specified by parameters and project the 3D component (or accumulated BIM) into 2D images, of which the number is same with the input photos. The image similarity is calculated as the SSIM index and returns CMA-ES as the objective value $f(X_i)$. The objective values can update the covariance matrix of CMA-ES for succeeding trials. Although each trial may not necessarily guarantee a higher SSIM, the evolution strategy of CMA-ES will achieve a higher SSIM eventually.

To scale up the trial-and-error procedure from one individual component to the overall as-built BIM generation, a two-stage strategy is adopted. Stage 1 aims to fit individual components into the as-built BIM one by one, following the topological relationships and constraints. The target BIM is thus incrementally generated by appending one component after another. Stage 2 is to refine the fitted
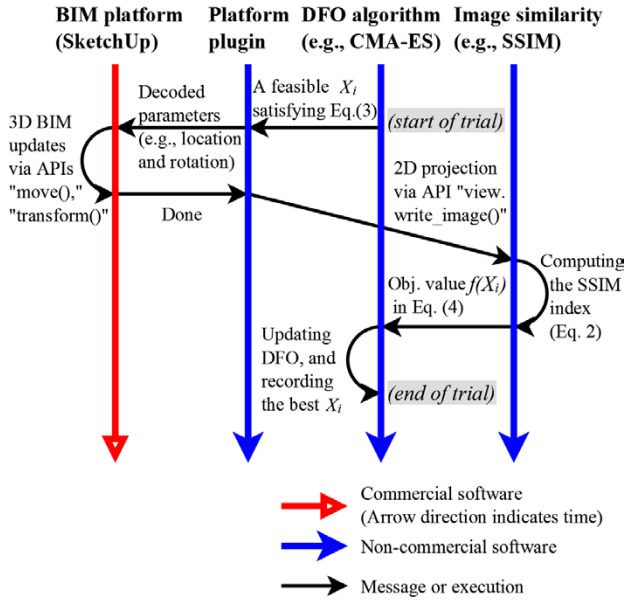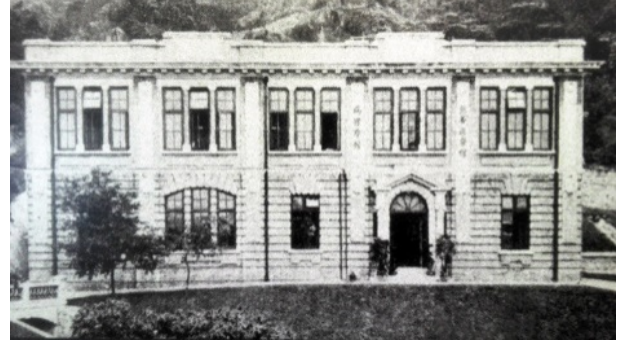
Figure 3 Message sequence chart of the operations and interactions between the modules of COBIMG in an individual trial

BIM holistically by fine-tuning the available components, to achieve a higher similarity between the BIM and the measurement. Both call the similar trials of COBIMG but the former is at individual component level on incomplete models while the latter is on complete models and may involve inter-component operations (e.g., swapping two components). The trials will continue until some termination conditions (e.g., the maximum number of trials) are met. The parameters that result in the best similarity amongst the trials is the final output. The generated as-built BIM is semantically rich based on two sources of information, i.e., online open libraries (for standard geometry, materials, and details) and DFO-based component fitting (for as-built position, scaling, rotation, and topological relationships).

4 EXPERIMENTAL TESTS

4.1 Experimental setting

In this study, the feasibility of the proposed as-built BIM generation method is validated through a somewhat extreme outdoor case and an indoor case (See Figure 4). In the outdoor case, the target building is The School of Tropical Medicine and School of Pathology of The University of Hong Kong (HKU), which used to be a baroque-style two-story building. As the building was built in 1919 and demolished more than two decades ago, it is almost impossible to collect the information of this building through laser scanning or other surveying technologies. The only information available is the photo provided by the HKU Estates Office, as shown in Figure 4(a). In this case, the proposed method is tested to generate the model from

(a) Outdoor case: A demolished building of The School of Tropical Medicine and School of Pathology, The University of Hong Kong (640×360 pixels; source: Archives of HKU Estates Office)

(b) Indoor case: A scene in a furniture store (384×512 pixels; taken by a smart phone camera with 28mm effective focal length; resolution down sampled)

Figure 4 An outdoor case and an indoor case for evaluating the proposed method

the single image. Specifically, apparent components with both width and height greater than 1.0 meter were required to be recognized and fitted in the BIM. The target BIM thus demanded a set of component instances including one door portico, one tree, two storeys of walls, and nine windows. The camera was approximately located at the position (0, 21.6, 4) (x, y, z in meter) pointing to (0, 0, 4) in SketchUp, based on a triangulation of the photo with the building footprint from a survey map of HKU in the period 1969~1976. The categories and the numbers of BIM components were given in the experiments: 1 Baroque style building, 2 storeys, 4 windows (of unknown classes) and 1 door on the G/F, 5 identical windows (of unknown classes) on the 1/F, 1 tree (of unknown classes) in front of the building. Except for the trees, the rotation parameters were omitted due to the photo having been properly shot from the front according to the triangulation.

The indoor case was a furniture scene with a few chairs in the corner, as shown in Figure 4(b). In this case, the input was two photos taken from different directions, where the cameras were with 28mm focal length and located at (2.12, 1.11, 1.50) pointing to (0, 1.06, 0.05) and (0.64, 2.69, 1.50)

Table 2
BIM components adopted from SketchUp 3D Warehouse

Id	Component		Original model from 3D Warehouse (Contributor ID)	Supplemented attributes of the component	
	category	class		As constraints	Not as constraints
–	Ground	Ground	–	–	–
The outdoor case	Door	Door portico	Door (3) Classical Ottoman Osmanli Colonial (*Mohamed EL Shahed*); Blenheim Orangery and Function Rooms (*Richard*)	Ranges of scaling; *contains_on* = Wall	IFC type and function; Materials;
	Tree	Oak tree	Downy Oak (KangaroOz 3D)	Ranges of scaling; range of *z*-rotation; *on_top_of* = Ground	*Ibid.*
		Palm tree	Royal Palm Tree (*Yoshi Productions*)	*Ibid.*	*Ibid.*
	Wall	With h-sliding	Salm Palace (*3dolomouc*)	Ranges of scaling; *on_top_of* = Ground	*Ibid.*
		Smooth surface	Salm Palace (*3dolomouc*)	Ranges of scaling; *on_top_of* = Wall	*Ibid.*
	Window	Three-section	French Window (*Architect*)	Ranges of scaling; *contains_on* = Wall	*Ibid.*
		Traditional	Mahogany Framed Window (*Ben*)	*Ibid.*	*Ibid.*
The indoor case	Chair	Armchair model *Vedbo*	VEDBO (*FRANKSON*)	Ranges of scaling; range of *z*-rotation; *on_top_of* = Ground	IFC type; Producer; Materials; Retail price;
		Armchair model *Villstad*	armchair (*tako*)	*Ibid.*	*Ibid.*
		Model *Kaustby*	IKEA - KAUSTBY (*Laurent B.*)	*Ibid.*	*Ibid.*
		Model *Nolmyra*	Nolmyra chair (*Jo E.*)	*Ibid.*	*Ibid.*
		Model *Norraryd*	NORRARYD (*Vera O.*)	*Ibid.*	*Ibid.*

point to (0, 0, 0.10), respectively. The ground truth included two armchairs (models *Vedbo* and *Villstad*) and a chair (model *Nolmyra*); the horizontal centers of the three chairs, measured by the authors with a tape, were (0.401, 0.524), (0.560, 1.343), and (0.381, 2.060), respectively. The task was to generate a BIM with three correct chairs and measure the error in terms of *root-mean-square deviation* (RMSD). The candidate BIM components were thus known as "chairs", but neither the types nor the numbers of the chairs were given in this case. Therefore, unlike following the given clues in the outdoor case, the COBIMG had to repeatedly try to place possible chair components till no better SSIM index can be found.

A set of BIM components, as listed in Table 2, were collected from 3D Warehouse of SketchUp with keyword filters "Baroque" and names of chair models. Topological constraints of the components listed in Table 1 were manually added as attributes in SketchUp. The attributes can be read and translated to the semantic constraints of the BIM components by the plugin of COBIMG. Some semantics that have not been associated with the constraints such as Industry Foundation Classes (IFC) types are also listed. The time of searching and downloading all the original models was about 24 minutes, the time of cleaning unnecessary parts from the components was about 45 minutes, and the annotation of the constraints cost about 22 minutes.

The experiments were conducted on a laptop computer with Intel i7 CPU (2.60 GHz), 16 GB RAM, and the Windows 10 64-bit operating system. The adopted DFO algorithm was CMA-ES and the adopted image similarity was the SSIM index. In each case, the as-built BIM generation started from an empty model with only one invisible 'Ground' component ($z = 0$). The BIM was incrementally generated by attaching one component each time, starting from those eligible to connect to the 'Ground' component. As a result, the 'Wall' components preceded the 'Windows' and 'Doors.' For fitting each component, a fixed number of trials of CMA-ES algorithm were allowed in the COBIMG. The number of trials was set from 10 to 2,000 in a sequence of seven values increasing exponentially.

4.2 The results of the outdoor case

The results of similarity, overall time cost, and correctly generated components observed from the outdoor case by changing different number of trials are shown in Figure 5. In general, both the similarity and overall time cost monotonically increased when the number of trials increased from 10 to 2,000. The similarity increased from about 0.16 to over 0.24, the time cost increased from a couple of minutes to about three hours, and the number of correctly generated instances of components in the generated model varied from 4/13 to 12/13. It was interesting to observe that some components were wrongly, but reasonably, generated. For example, in the generated model from 200 trials for each component, the oak tree component was wrongly fitted into a similar presence of a
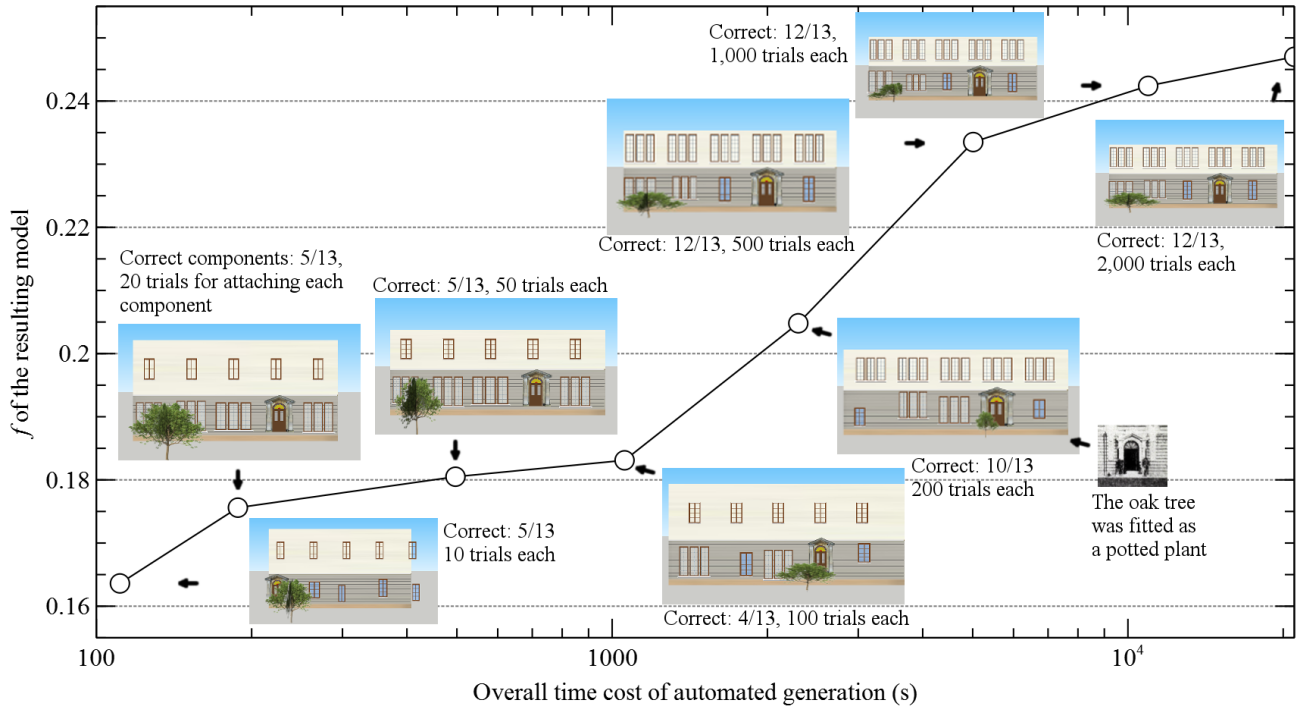
Figure 5 The trends of similarity, overall time cost, and correctly generated components in the outdoor case when changing the trials of CMA-ES for fitting each component
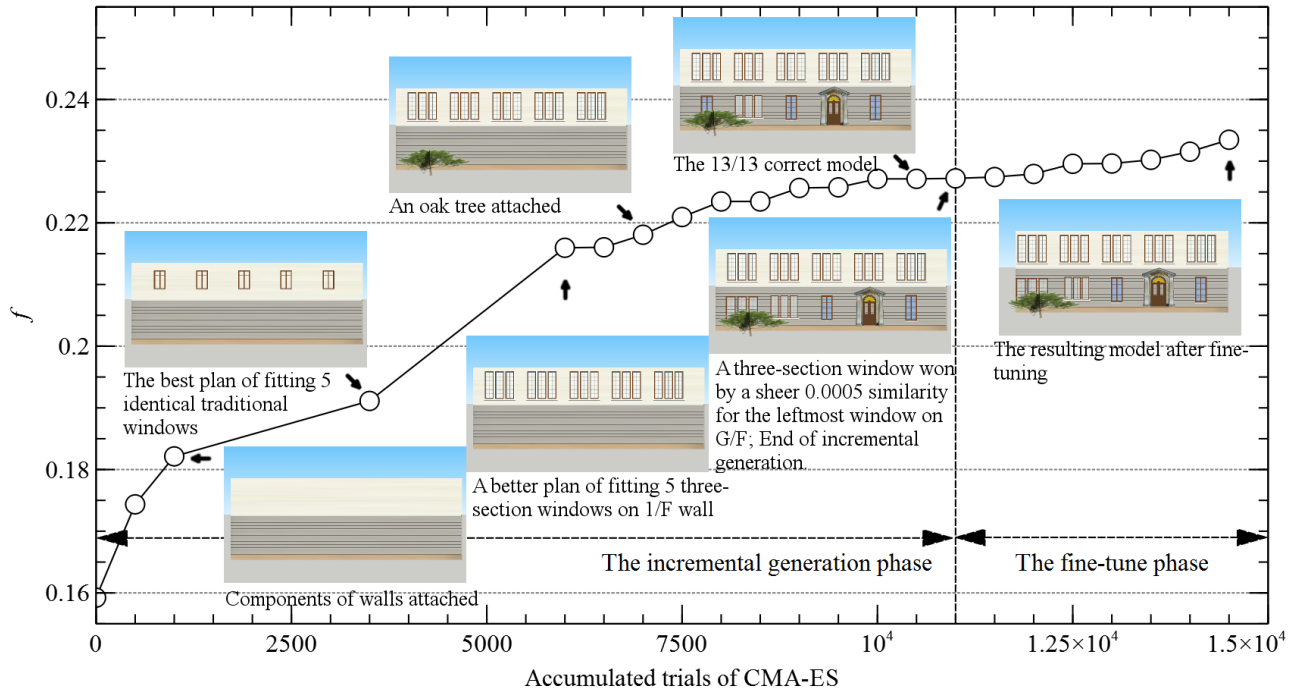

Figure 6 The automated optimization process of the proposed method with annotated SketchUp models for the outdoor case with 500 trials for fitting each component

potted plant in front of the door. By comparing the trade-offs between the number of correctly generated components and the time cost, 500 trials are suitable for generating a satisfactory result under the given experimental settings.

The number 500 also fell in the suggested range of evaluations (i.e., at least 100) of CMA-ES (Hansen, 2016).

Figure 6 illustrates the detailed BIM generation procedure of the test in which the number of trials was set

(a) Auto-generated front face by the proposed method in SketchUp

(b) Manually completed building model

Figure 7 The generated model in the test with 500 trials for fitting each component

to 500. After the first 500 trials, the G/F wall was attached to the model, and after another 500 trials the 1/F wall was attached to the model. Then a group of five identical traditional windows were attached and later replaced by another group of five three-section windows, because the prior group's contribution was only $f = 0.1921$ whereas the later option's contribution was much better at $f = 0.2165$. The incremental generation phase stopped at the 11,000th trial. After another 3,500 trials of the fine-tuning phase, the final model achieved a fitness of $f = 0.2335$ by slightly changing the locations and scales of the components automatically. Although 12 out of 13 components were correctly generated, it can be seen that all 13 components were once correctly put together at the 10,500 of accumulated trials but that the leftmost window on G/F was replaced due to a slight 0.0005 improvement of similarity. The overall time was 1 hour 23 minutes and 32.6 seconds (5,012.6s). The result of the proposed method was saved as a 2.2 MB SketchUp file.

As some components in the generated model did not perfectly match the given baroque architecture, such as a three-section window on the G/F, the authors made a few manual amendments to the auto-generated front face of the building. Figures 7(a) and 7(b) show the window example highlighted with red circles. The model of the whole building, as shown in Figure 7(b), was estimated based on the survey map of HKU and manually completed with replicas of the auto-generated facade.

The resulting model integrated rich semantic information from two resources. The proposed method generated the geometric information of location, scaling, and rotation for each component, as well as topological relationships. Some other semantic information, such as functions and materials, was inherited from the component set. Figure 8 shows a screenshot of the semantics for a window component, including the IFC type, parent component (i.e., the exterior wall on 1/F), storey, as attributes in the generated model.
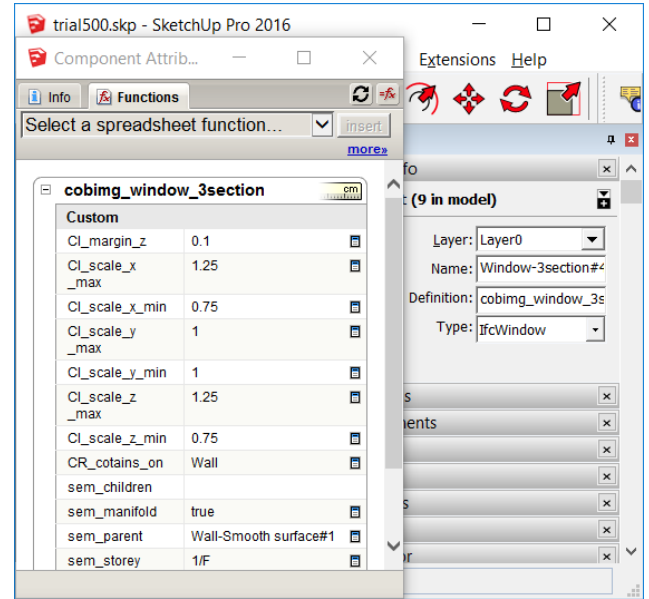

Figure 8 Semantics as attributes of a window in the generated model

4.3 The results of the indoor case

Figure 9 shows the results of similarity, overall time cost, and correctly generated components observed from the indoor case by changing the number of trials in the indoor case: The similarity increased from about 0.62 to about 0.68 when the number of trials per component changed from 10 to 2,000. During the incremental of trials, the number of correctly generated instances of components in the generated model varied from 1/3 to 3/3, the error (i.e., RMSD) reduced from over 40 cm to less than 5 cm, yet the time cost increased from less than 1 minute to over five hours. It can be found from Figure 9 that a very small part of the headrest of the *Vedbo* chair was buried in the wall in many resulting models, as highlighted by the circles. This was because the real chair was bendable when leaning on a wall, but the shapes of BIM components on SketchUp and most modern BIM platforms are rigid. Similar to the number of trials in the outdoor case, 500 are also suitable for a satisfactory result under the given settings.

Figure 10 illustrates the details in the BIM generation procedure of the test in which the number of trials was set to 500. There were totally 11,500 trials, which consisted of 10,000 trials in the incremental generation phase in four rounds and 1,500 trials in the fine-tune phase. In the first round, the best component was a *Vedbo* armchair with a fitness of $f = 0.6437$, and the next best one was a *Villstad* armchair with a fitness of $f = 0.6185$. Thereafter, the *Vedbo* armchair was placed in the model. In the second round, a *Villstad* armchair retuned the highest fitness $f = 0.6694$, and was thus placed next to *Vedbo*. The third chair was a *Nolmyra* chair with a slightly better fitness $f = 0.6706$. No better fitness (i.e., SSIM index) was found during the trials of attaching the fourth chair. Hence, the incremental
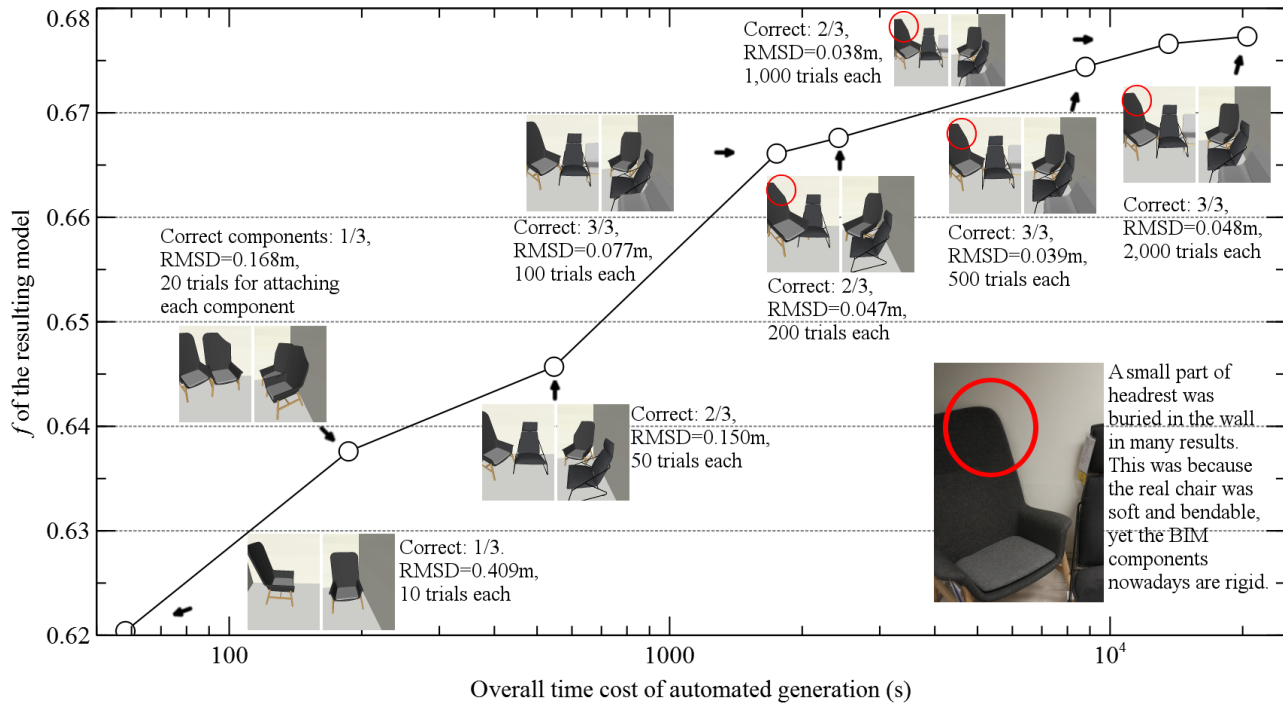
Figure 9 The trends of similarity, overall time cost, and correctly generated components in the indoor case when changing the trials of CMA-ES for fitting each component
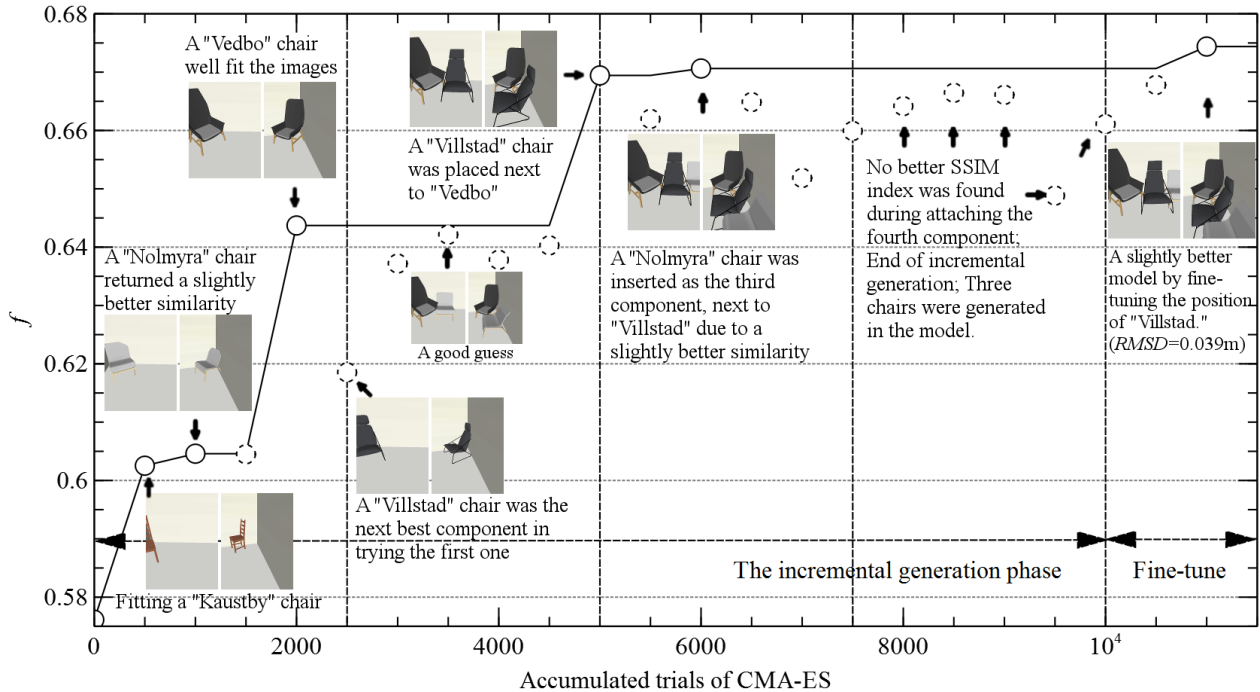

Figure 10 The automated optimization process of the proposed method with annotated SketchUp models for the indoor case with 500 trials for fitting each component

generation phase of COBIMG ended and the model contains three chairs. In the fine-tune phase, the BIM was updated by a slightly better fitness $f = 0.6744$. The three chairs in the resulting BIM were all correct and with an RMSD of 3.9 cm. The error level was acceptable, because the downloaded component models including *Vedbo* and *Nolmyra* were not exactly the same as the latest chair models. The overall time was 2 hour 26 minutes and 32.9
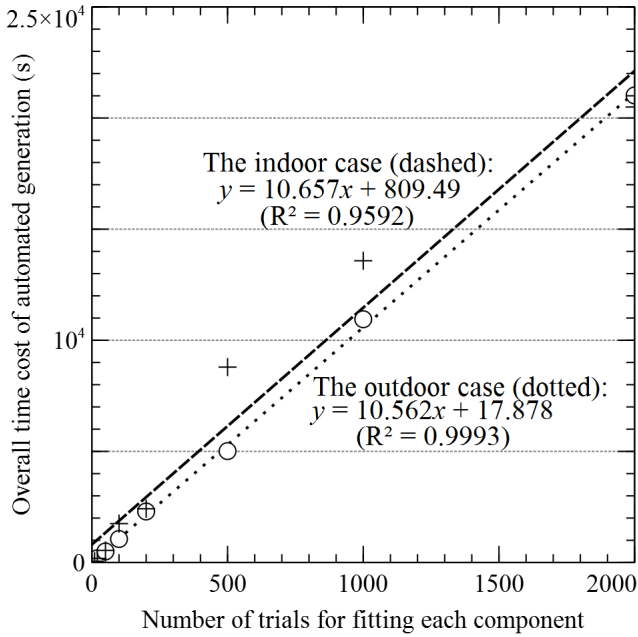
Figure 11 The linear relationship between overall time cost and the number of trials in both cases

Table 3
Computing resource consumption breakdown in the tests with 500 trials in both cases

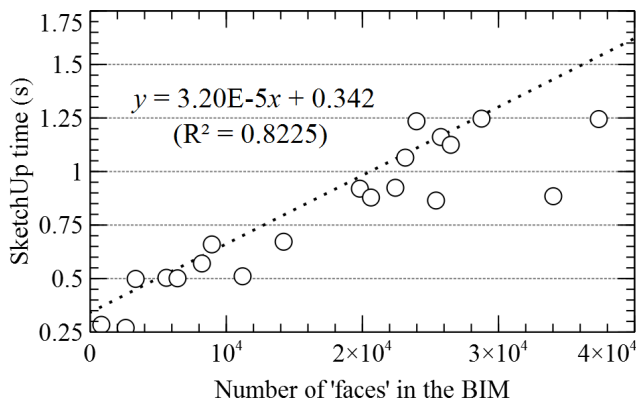| Used by	Functions	% of time	
		Outdoor	Indoor
SketchUp & plugin	Manipulating components; 3D to 2D projection	97.67%	97.78%
Similarity to the input	Computing the image similarity index	1.45%	1.33%
DFO algorithm	Optimizing the parameters of a component	0.00%	0.00%
System/disk	Reading/writing of logs and temporary image files	0.88%	0.89%

Figure 12 The strong correlation between the computational time spent by SketchUp and the number of 'faces' in the BIM to manipulate and project (Note: *Pearson's cor.* = 0.907, $p < 0.0001$, two-tailed)

seconds (8,792.9s). The result of the proposed method was saved as a 13.0 MB SketchUp file.

4.4 The computational time

The overall time cost in both cases increased in a linear relationship with the number of trials per component, as shown in Figure 11. The linear relationship was more convincing ($R^2 = 0.9993$) in the outdoor case than that ($R^2 = 0.9592$) in the indoor case, because the number of components was unknown in the tests of the latter case. In fact, the incremental procedure of component fitting also indicates that the overall time cost is in a linear relationship with the total number of candidate components in the libraries. Therefore, one can expect a linear increment on time cost when setting up more candidate components (e.g., more models of chairs). Table 3 lists the breakdown of computational time spent by different modules of COBIMG. It can be found from Table 3 that over 95% of the time was, in both cases, spent by SketchUp manipulating components and projecting the model from 3D to 2D. Further bivariate analysis of the experimental data showed that the computational time spent by SketchUp had a *significant strong positive* correlation (*Pearson's correlation* = 0.907, $p < 0.0001$, two-tailed) with the number of 'faces' in the BIM to manipulate and project. Figure 12 illustrates the correlation and an equation by linear regression, which indicates about 30,000 more 'faces' would increase the SketchUp time by one second under the experimental settings.

5 DISCUSSION

5.1 Advantages and shortcomings of the proposed method

The proposed DFO approach has been identified through experimentation to have the following advantages over conventional laser scanning and photogrammetry based methods:

1. The proposed approach does not engage in the burdensome task of preprocessing and segmenting the as-built measurement (e.g., point cloud or images captured by laser scanning or photogrammetry) but rather regards the measurement as an entity so that no explicit object recognition processes are introduced; it directly compares the similarity between the target measurement and the image from projecting the BIM model. Eliminating object recognition processes increases the computational load (owing to the larger solution space), but advanced algorithms and powerful computers can handle this.

2. The data requirement is much more relaxed than developing a BIM model from laser scanning or photogrammetry. As illustrated in the experiment,

the BIM of the building facade can be automatically developed from one single image.

3. Compared with existing semi-automatic methods, which consist of automatic segmentation and manual semantics enrichment, the proposed method can make use of extensively available BIM object resources over the Internet so that less human intervention is needed. This capacity epitomizes the novel idea proposed in this paper of enriching BIM semantics by dealing with the dilemma of information inadequacy and information overload when generating a BIM.

4. The proposed method adopts mature fitness function from the field of computer vision and pattern recognition; it has a high scalability to new environments even without adjusting the configuration of the fitness function.

5. The innovative and interdisciplinary application of established DFO in semantically rich as-built BIMs opens a whole new avenue for the worldwide business of generating as-built BIMs.

Although the method proposed in this study has many merits, it also has the following shortcomings:

1. The quality of the outcome is highly dependent on the availability of components. For buildings that have irregular components, an extra manual effort is needed to tailor the specifically required components, such as historical BIM objects (Dore and Murphy, 2014; Santagati and Turco, 2017), before applying the proposed method. Thanks to online open BIM vendors, building modelers, and many industrial practitioners who contribute to the richness of the existing BIM component libraries, it can be expected that the availability of BIM components will not be a serious problem in implementing the proposed method.

2. The proposed method allows BIM model generation from one single image, but the level of accuracy (e.g., centimeter-accuracy) may not be as high as a model generated from laser scanning or photogrammetry (e.g., millimeter-accuracy), and the building components that are not shown or invisible (e.g., joints or beams inside a wall) in the image cannot be automatically modeled. One way to compensate for this is to use multiple images taken from various angles for calibration.

3. The computer program cannot compare with BIM modelers' professional knowledge, experience, and insights in model generation. There is a tradeoff amongst the costs of data input, automation/human intervention level, and the level of semantic richness in as-built BIM generation.

5.2 Future developments

Although this paper has focused on 2D imagery input using the SSIM as the similarity index measurement and the CMA-ES as the DFO solver, the proposed method can incorporate more inputs and computation. For example, in addition to individual images, the DFO approach can also accept point clouds or processed imagery, as long as their data collection costs are affordable. If the input is point clouds, the objective function/similarity measurement could be more complicated. For example, the MSE can be used to measure Euclidean distance and difference of color between an as-built BIM and an input point cloud. It has yet to be determined which similarity index is more effective than another for a certain type of data input.

In solving the constrained optimization problem, many well-known computational algorithms, such as surrogate methods and trust region methods, can also be adopted with acceptable performance. The multimodality of optimal solutions was also observed in the experiments. However, it is so far unclear whether the performance of these DFO algorithms and other multimodal algorithms are satisfactory for constructing as-built BIMs.

It is noteworthy that some simple architecture conventions have been translated into constraints such as building style, topological relationships, and feasible scale range, which can significantly improve the efficiency of the DFO approach for as-built BIM generation. These architecture conventions are not accidental, but often the result of economical, manufacturing, functional, or aesthetic considerations (Mitra and Pauly, 2008). Some of the conventions can be obtained from ordinances or standards, while others can be originated from general observation in real-world situations (e.g., Chen et al., 2017). These should be further explored and formalized for computer vision and pattern recognition, with a focus on their applications in as-built BIM generation.

In this paper, as-built BIM generation is formulated as a constrained optimization problem. In solving the problem, a specific platform, Trimble SketchUp, and BIM components compatible with the platform are chosen. Other platforms such as Autodesk Revit should be explored in the future. Results of the experimental tests conducted in this study confirm that by consuming over 95% of the time, the current single-thread BIM platform is the bottleneck in applying the proposed method. Taking advantage of up-to-date multi-threading and GPUs could lead to a breakthrough in the wide adoption of the proposed method. In addition, this research preliminarily explored generated BIMs with the IFC standard, but the actual interoperability has yet to be ascertained and could be the subject of future studies.

In summary, the use of a derivative-free optimization (DFO) approach to the generation of semantically rich as-built BIMs is a seminal idea that this research has brought to fruition with satisfactory results. However, there are

many areas such as required inputs, variable settings, objective functions, constraints, software platforms, output formats, and performance measurements of the constrained optimization problem that need further development.

6 CONCLUSION

This paper developed a novel DFO method for semantically rich as-built BIM generation. It started from the dilemma of information inadequacy and information overload in BIM generation: on the one hand, there is a lack of semantic information in the as-built BIMs, while on the other hand there is plenty of semantics in various open-access BIM components to be fully exploited. The approach translated the as-built BIM generation into a constrained optimization problem, whereby advanced DFO algorithms, augmented with some architecture constraints, were applied to recognize the best combination of BIM components from the data input (i.e., measurement of as-built conditions). The recognized BIM was further linked with existing BIM component libraries as a cost-effective way to enrich the semantics. The originality of this research is in challenging prevalent practice by introducing the as-built BIM generation as a rigorous mathematical formulation with considerable computational complexity.

The DFO method was prototyped in this study through a series of rigorous tests, which were conducted as an extreme experiment where a semantically rich as-built BIM was satisfactorily generated from a single photo of a demolished building. The experiment confirmed that the DFO approach is effective for as-built BIM generation regarding time efficiency and semantic richness. Limitations of the proposed method, including the dependency on BIM component libraries and the quality of the generated model, were also identified. The research team intends to undertake further research to validate other advanced algorithms, different input measurements, parallel computation, and more semantic-based constraints and reasoning.

The research described in this paper is of theoretical and practical significance. It validates the theoretical foundation for transferring the generation of an as-built BIM to a nonlinear optimization problem, while challenging the segmentation of measurement data in prevailing approaches. Facility developers around the world are demanding as-built BIMs as a deliverable, and the current way of meeting this demand is by using expensive technologies such as laser scanning, photogrammetry, and SLAM. The DFO approach introduced in this paper could be a game changer in the competitive landscape of the BIM business. The approach can also make invaluable contributions to heritage conservation, smart city development, and environmental protection.

REFERENCES

Adan, A. & Huber, D. (2011), 3D reconstruction of interior wall surfaces under occlusion and clutter. In *2011 International Conference on 3D Imaging, Modeling, Processing, Visualization and Transmission (3DIMPVT 2011)*, pp. 275-281, Hangzhou, China. doi:10.1109/3DIMPVT.2011.42

Adeli, H. & Cheng, N. T. (1994). Concurrent genetic algorithms for optimization of large structures. *Journal of Aerospace Engineering*, **7**(3), 276-296.

Adeli, H. & Kamal, O. (1986). Efficient optimization of space trusses. *Computers & Structures*, **24**(3), 501-511.

Adeli, H. & Kumar, S. (1995). Concurrent structural optimization on massively parallel supercomputer. *Journal of Structural Engineering*, **121**(11), 1588-1597.

Andreopoulos, A. & Tsotsos, J. K. (2013), 50 years of object recognition: Directions forward. *Computer Vision and Image Understanding*, **117**(8), 827-891.

Anil, E. B., Tang, P., Akinci, B. & Huber, D. (2013), Deviation analysis method for the assessment of the quality of the as-is Building Information Models generated from point cloud data. *Automation in Construction*, **35**, 507-516.

Aster, R. C., Borchers, B. & Thurber, C. H. (2013). *Parameter estimation and inverse problems*. 2nd Ed. Academic Press, Oxford, UK.

Athanasiou, A., De Felice, M., Oliveto, G. & Oliveto, P. S. (2011). Evolutionary algorithms for the identification of structural systems in earthquake engineering. In *Proceedings of the International Conference on Evolutionary Computation Theory and Applications - Volume 1: ECTA, (IJCCI 2011)*, pp. 52-62. doi:10.5220/0003672900520062

Babacan, K., Chen, L. & Sohn, G. (2017). Semantic Segmentation of Indoor Point Clouds Using Convolutional Neural Network. *ISPRS Annals of Photogrammetry, Remote Sensing and Spatial Information Sciences*, **IV-4/W4**, 101-108.

Becerik-Gerber, B., Jazizadeh, F., Li, N. & Calis, G. (2011), Application areas and data requirements for BIM-enabled facilities management. *Journal of Construction Engineering and Management*, **138**(3), 431-442.

Belsky, M., Sacks, R. & Brilakis, I. (2016), Semantic enrichment for building information modeling. *Computer-Aided Civil and Infrastructure Engineering*, **31**(4), 261-274.

Bosché, F., Ahmed, M., Turkan, Y., Haas, C. T. & Haas, R. (2015), The value of integrating Scan-to-BIM and Scan-vs-BIM techniques for construction monitoring using laser scanning and BIM: The case of cylindrical MEP components. *Automation in Construction*, **49**, 201-213.

Cantzler, H. (2003), *Improving architectural 3D reconstruction by constrained modelling* (PhD thesis, University of Edinburgh, Edinburgh, UK), Retrieved from http://hdl.handle.net/1842/319

Chen, K., Lu, W., Peng, Y., Rowlinson, S. & Huang, G. Q. (2015), Bridging BIM and building: From a literature review to an

integrated conceptual framework. *International Journal of Project Management*, **33**(6), 1405-1416.

Chen, K., Xue, F. & Lu, W. (2017), Development of 3D building models using multi-source data: A study of high-density urban area in Hong Kong. In *Proceedings of Lean & Computing in Construction Congress (LC3 2017)*, pp. 609-616. Heraklion, Greece. doi:10.24928/JC3-2017/0252

Cho, Y. K., Ham, Y. & Golpavar-Fard, M. (2015), 3D as-is building energy modeling and diagnostics: A review of the state-of-the-art. *Advanced Engineering Informatics*, **29**(2), 184-195.

Clancey, O. & Witten, M. (2011), A memetic algorithm for dosimetric optimization in CyberKnife robotic radiosurgical treatment planning. In *Proceedings of the 2011 IEEE Congress on Evolutionary Computation (CEC 2011)*, pp. 880-885.

Conn, A. R., Scheinberg, K. & Vicente, L. N. (2009), *Introduction to derivative-free optimization*, SIAM, Philadelphia, PA, USA.

Criminisi, A., Reid, I. & Zisserman, A. (2000), Single view metrology. *International Journal of Computer Vision*, **40**(2), 123-148.

Dai, F. & Lu, M. (2010), Assessing the accuracy of applying photogrammetry to take geometric measurements on building products. *Journal of Construction Engineering and Management*, **136**(2), 242-250.

Díaz-Vilariño, L., Conde, B., Lagüela, S. & Lorenzo, H. (2015), Automatic detection and segmentation of columns in as-built buildings from point clouds. *Remote Sensing*, **7**(11), 15651-15667.

Dimitrov, A., Gu, R. & Golparvar-Fard, M. (2016), Non-uniform B-spline surface fitting from unordered 3D point clouds for as-built modeling. *Computer-Aided Civil and Infrastructure Engineering*, **31**(7), 483-498.

Dore, C. & Murphy, M. (2014), Semi-automatic generation of as-built BIM facade geometry from laser and image data. Journal of Information Technology in Construction (ITcon), **19**(2), 20-46.

Eastman, C. M., Teicholz, P., Sacks, R. & Liston, K. (2011), *BIM handbook: A guide to building information modeling for owners, managers, designers, engineers and contractors*, 2nd Edition. John Wiley & Sons, Hoboken, New Jersey, USA.

Eiben, A. E. & Smith, J. E. (2003), *Introduction to evolutionary computing*, Springer, Heidelberg.

Faber, P. & Fisher, B. (2002), How can we exploit typical architectural structures to improve model recovery?. In *Proceedings of First International Symposium on 3D Data Processing Visualization and Transmission*, pp. 824-833. doi:10.1109/TDPVT.2002.1024167

Fisher, R. B. (2004). Applying knowledge to reverse engineering problems. *Computer-Aided Design*, **36**(6), 501-510.

Gill, P. E., Murray, W. & Wright, M. H. (1981), *Practical optimization*. Academic Press, London.

Hamledari, H., Rezazadeh Azar, E. & McCabe, B. (2017). IFC-based development of as-built and as-is BIMs using construction and facility inspection data: Site-to-BIM data transfer automation. *Journal of Computing in Civil Engineering*, **32**(2), 04017075.

Hansen, N. (2016). The CMA evolution strategy: A tutorial. arXiv preprint, arXiv:1604.00772. https://arxiv.org/abs/1604.00772

Hansen, N., Auger, A., Ros, R., Finck, S. & Pošík, P. (2010). Comparing results of 31 algorithms from the black-box optimization benchmarking BBOB-2009. In *Proceedings of the 12th annual conference companion on Genetic and evolutionary computation*, pp. 1689-1696. doi:10.1145/1830761.1830790

Hansen, N. & Ostermeier, A. (2001), Completely derandomized self-adaptation in evolution strategies. *Evolutionary Computation*, **9**(2), 159-195.

Henry, P., Krainin, M., Herbst, E., Ren, X. & Fox, D. (2012). RGB-D mapping: Using Kinect-style depth cameras for dense 3D modeling of indoor environments. *The International Journal of Robotics Research*, **31**(5), 647-663.

Holgado-Barco, A., Riveiro, B., González-Aguilera, D. & Arias, P. (2017). Automatic inventory of road cross-sections from mobile laser scanning system. *Computer-Aided Civil and Infrastructure Engineering*, **32**(1), 3-17.

Houshiar, H. & Nüchter, A. (2015). 3D point cloud compression using conventional image compression for efficient data transmission. In *Proceedings of the 2015 XXV International Conference on Information, Communication and Automation Technologies (ICAT)*, pp. 1-8. IEEE. doi:10.1109/ICAT.2015.7340499

Ilter, D. & Ergen, E. (2015), BIM for building refurbishment and maintenance: Current status and research directions. *Structural Survey*, **33**(3), 228-256.

Jung, J., Hong, S., Jeong, S., Kim, S., Cho, H., Hong, S. & Heo, J. (2014). Productive modeling for development of as-built BIM of existing indoor structures. *Automation in Construction*, **42**, 68-77.

Kaveh, A., Kalateh-Ahani, M. & Masoudi, M. S. (2011). The CMA evolution strategy based size optimization of truss structures. *International Journal of Optimization in Civil Engineering*, **1**(2), 233-56.

Koo, C., Hong, T., Yoon, J. & Jeong, K. (2016). Zoning-based vertical transportation optimization for workers at peak time in a skyscraper construction. *Computer-Aided Civil and Infrastructure Engineering*, **31**(11), 826-845.

Koppula, H. S., Anand, A., Joachims, T. & Saxena, A. (2011). Semantic labeling of 3d point clouds for indoor scenes. In *Advances in Neural Information Processing Systems 24*, pp. 244-252. Available at: http://papers.nips.cc/paper/4226-semantic-labeling-of-3d-point-clouds-for-indoor-scenes.pdf

Lagüela, S., Díaz-Vilariño, L., Martínez, J. & Armesto, J. (2013). Automatic thermographic and RGB texture of as-built BIM for energy rehabilitation purposes. *Automation in Construction*, **31**, 230-240.

Lee, D. S., Gonzalez, L. F., Periaux, J. & Srinivas, K. (2008), Robust design optimisation using multi-objective evolutionary algorithms. *Computers & Fluids*, **37**(5), 565-583.

Li, W., Pu, H., Schonfeld, P., Yang, J., Zhang, H., Wang, L. & Xiong, J. (2017). Mountain railway alignment optimization with bidirectional distance transform and genetic algorithm. *Computer-Aided Civil and Infrastructure Engineering*, **32**(8), 691-709.

Mitra, N. J. & Pauly, M. (2008), Symmetry for architectural design. In *Advances in Architectural Geometry (AAG2008)*, pp. 13-16. Available at: http://www.architecturalgeometry.org/aag08/aag08proceedings-papers_and_poster_abstracts.pdf

National Institute of Building Sciences (NIBS) (2015), *National Building Information Modeling Standard.* Version 3, Retrieved from https://www.nationalbimstandard.org/

Nex, F. & Remondino, F. (2014), UAV for 3D mapping applications: A review. *Applied Geomatics*, **6**(1), 1-15.

Nguyen, T. H., Oloufa, A. A. & Nassar, K. (2005), Algorithms for automated deduction of topological information. *Automation in Construction*, **14**, 59-70.

Nicosia, G. & Stracquadanio, G. (2008), Generalized pattern search algorithm for peptide structure prediction. *Biophysical Journal*, **95**(10), 4988-4999.

Nüchter, A. (2009), *3D robotic mapping: The simultaneous localization and mapping problem with six degrees of freedom*, Springer-Verlag, Berlin, Heidelberg.

Schnabel, R., Wahl, R. & Klein, R. (2007), Efficient RANSAC for point-cloud shape detection. *Computer Graphics Forum*, **26**(2), 214-226. doi:10.1111/j.1467-8659.2007.01016.x

Pătrăucean, V., Armeni, I., Nahangi, M., Yeung, J., Brilakis, I. & Haas, C. (2015), State of research in automatic as-built modelling. *Advanced Engineering Informatics*, **29**(2), 162-171.

Perez-Perez, Y., Golparvar-Fard, M. & El-Rayes, K. (2016), Semantic and geometric labeling for enhanced 3D point cloud segmentation. In *Proceedings of Construction Research Congress 2016*, pp. 2542-2552. doi:10.1061/9780784479827.253

Quintana, B., Prieto, S. A., Adán, A. & Bosché, F. (2018). Door detection in 3D coloured point clouds of indoor environments. *Automation in Construction*, **85**, 146-166.

Sacks, R., Ma, L., Yosef, R., Borrmann, A., Daum, S. & Kattel, U. (2017). Semantic enrichment for building information modeling: Procedure for compiling inference rules and operators for complex geometry. *Journal of Computing in Civil Engineering*, **31**(6), 04017062.

Santagati, C. & Turco, M. L. (2017), From structure from motion to historical building information modeling: Populating a semantic-aware library of architectural elements. *Journal of Electronic Imaging*, **26**(1), 011007.

Snavely, N., Seitz, S. M. & Szeliski, R. (2008), Modeling the world from internet photo collections. *International Journal of Computer Vision*, **80**(2), 189-210.

Song, M., Shen, Z. & Tang, P. (2014), Data quality-oriented 3D laser scan planning. In *Proceedings of Construction Research Congress 2014*, pp. 984-993. doi:10.1061/9780784413517.101

Tang, P., Huber, D., Akinci, B., Lipman, R. & Lytle, A. (2010), Automatic reconstruction of as-built building information models from laser-scanned point clouds: A review of related techniques. *Automation in Construction*, **19**(7), 829-843.

Valero, E., Adán, A. & Cerrada, C. (2012), Automatic method for building indoor boundary models from dense point clouds collected by laser scanners. *Sensors*, **12**(12), 16099-16115.

Wang, C., Peng, Y., Cho, Y. & Li, H. (2011), As-built residential building information collection and modeling methods for energy analysis. In *Proceedings of the 28th International Symposium on Automation and Robotics in Construction (ISARC)*, Seoul, Korea, pp. 227-232. Available at: http://www.irbnet.de/daten/iconda/CIB_DC23633.pdf

Wang, Q., Cheng, J. C. & Sohn, H. (2017). Automated estimation of reinforced precast concrete rebar positions using colored laser scan data. *Computer-Aided Civil and Infrastructure Engineering,* **32**, 787-802.

Wang, Z., Bovik, A. C., Sheikh, H. R. & Simoncelli, E. P. (2004), Image quality assessment: From error visibility to structural similarity. *IEEE Transactions on Image Processing*, **13**(4), 600-612.

Wang, Z. & Simoncelli, E. P. (2008), Maximum differentiation (MAD) competition: A methodology for comparing computational models of perceptual quantities. *Journal of Vision*, **8**(12), 8.

Xiong, X., Adan, A., Akinci, B. & Huber, D. (2013), Automatic creation of semantically rich 3D building models from laser scanner data. *Automation in Construction*, **31**, 325-337.

Xiong, X. & Huber, D. (2010), Using Context to Create Semantic 3D Models of Indoor Environments. In *Proceedings of the 21st British Machine Vision Conference* (*BMVC2010)*, pp. 1-11.

Zhang, C., Kalasapudi, V. S. & Tang, P. (2016), Rapid data quality oriented laser scan planning for dynamic construction environments. *Advanced Engineering Informatics*, **30**(2), 218-232.

Zhang, G., Vela, P. A., Karasev, P. & Brilakis, I. (2015), A Sparsity-Inducing Optimization-Based Algorithm for Planar Patches Extraction from Noisy Point-Cloud Data. *Computer-Aided Civil and Infrastructure Engineering*, **30**(2), 85-102.

Zhu, X. X. & Shahzad, M. (2014). Facade reconstruction using multiview spaceborne TomoSAR point clouds. *IEEE Transactions on Geoscience and Remote Sensing*, **52**(6), 3541-3552.